S1 Isoprene-to-monoterpene emission ratios

Figure S1 shows the isoprene-to-monoterpene molar emission ratios of the MEGAN-MOHYCAN inventory for 2019. In SICMA, an emission ratio of factor 10 is assumed. Deviations to this number, as shown by blue and red regions in Fig. S1, will result in different HCHO yields compared to full chemistry runs. In blue regions, monoterpene emissions are higher than assumed in SICMA, leading to an underestimation of the HCHO yield in SICMA and too high OH concentrations due to the lack of monoterpene oxidation. In red regions, monoterpene emissions are lower than assumed, which generally implies too high HCHO yields from SICMA. The spatial distribution of the emission ratios therefore shows many similarities to the HCHO column difference map (in BVOC dominated regions), shown in Fig. 4c of the main paper.

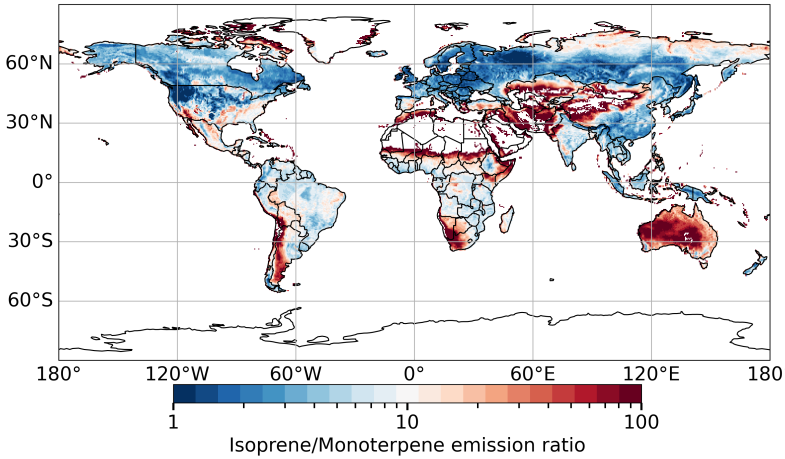

Figure S1. Isoprene-to-monoterpene emission ratios from MEGAN-MOHYCAN (Stavrakou et al., 2018) in 2019 in terms of molecules emitted.

S2 Top-down anthropogenic and pyrogenic VOC emissions

Figure S2 shows the a priori and optimized biomass burning VOC emissions, as well as the emission enhancement ratios, for 2019. The emissions have been regridded to the resolution of the model (i.e. $2° \times 2.5°$). The emission inversion suggests $\sim 5\%$ higher emissions compared to the bottom-up inventory, increasing the global total from 92.6 to 98.5 Tg VOC. The largest enhancement is found for the Siberian fires of 2019, where the observed TROPOMI HCHO columns are high (Fig. 1 of the main paper).

The a priori and optimized emission maps for anthropogenic VOCs are shown in Fig. S3. The optimized anthropogenic VOC emissions are roughly 20% higher (158.9 Tg vs. 198.6 Tg). The main enhancements with respect to the bottom-up emissions are located in Asian countries, i.e. Iran, India, and China. Since these countries are already significant emitters of anthropogenic VOCs, the impact on the global totals is relatively large.

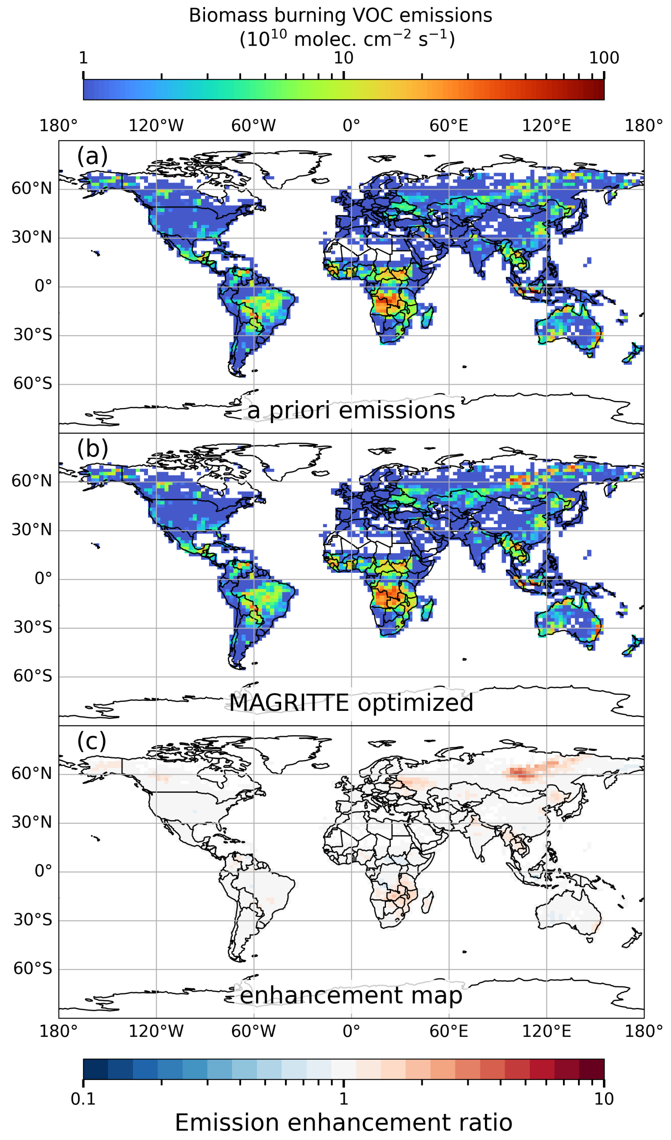

Figure S2. Biomass burning VOC emissions from QFEDv2.4 (Darmenov and da Silva, 2015, panel a), and derived from an emission inversion using the MAGRITTEv1.2 chemistry (b), averaged for the year 2019. Panel (c) shows the emission enhancement map, calculated as the ratio of panel (b) over panel (a).

References

Darmenov, A. and da Silva, A.: The Quick Fire Emissions Dataset (QFED): Documentation of versions 2.1, 2.2 and 2.4, NASA Technical Report Series on Global Modeling and Data Assimilation NASA TM-2015-104606, 38, 2015.

Soulie, A., Granier, C., Darras, S., Zilbermann, N., Doumbia, T., Guevara, M., Jalkanen, J.-P., Keita, S., Liousse, C., Crippa, M., Guizzardi, D., Hoesly, R., and Smith, S. J.: Global Anthropogenic Emissions (Cams-Glob-Ant) For The Copernicus Atmosphere Monitoring Service Simulations Of Air Quality Forecasts And Reanalyses, Earth System Science Data, 16, 2261–2279, https://doi.org/10.5194/essd-16-2261-2024, 2024.

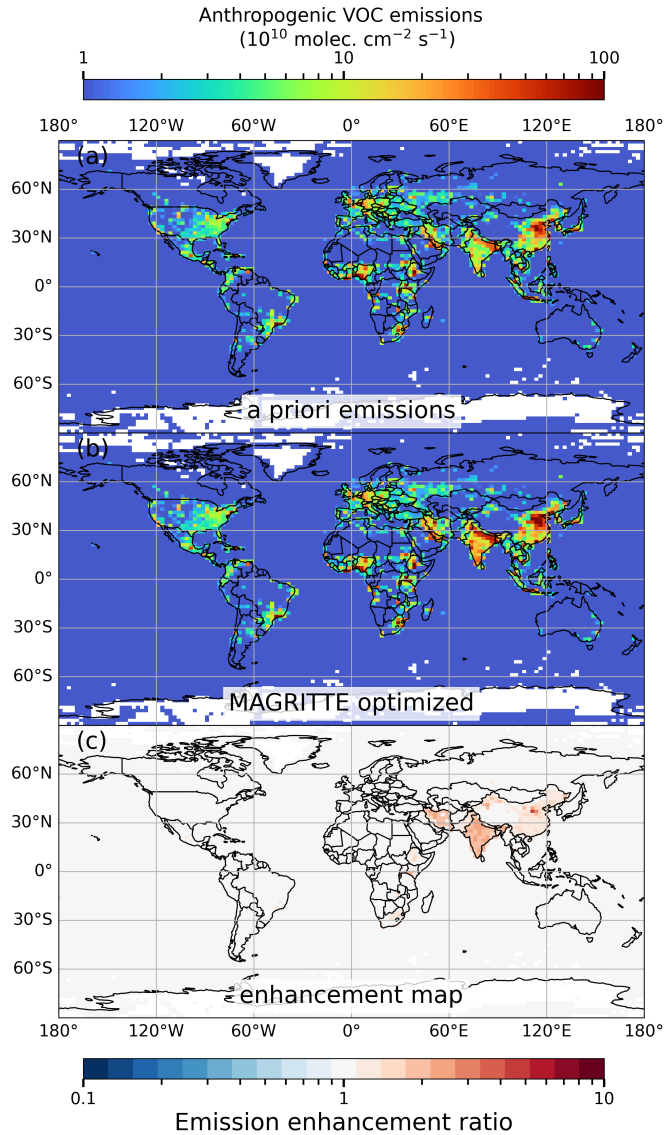

Figure S3. Same as Fig. S2, but for anthropogenic VOC emissions. A priori emissions (panel a) are taken from CAMS-GLOB-ANTv5.3 (Soulie et al., 2024).

Stavrakou, T., Müller, J. F., Bauwens, M., De Smedt, I., Van Roozendael, M., and Guenther, A.: Impact of Short-Term Climate Variability on Volatile Organic Compounds Emissions Assessed Using OMI Satellite Formaldehyde Observations, Geophys. Res. Lett., 45, 8681–8689, https://doi.org/10.1029/2018GL078676, 2018.